ADVANCES IN ATMOSPHERIC SCIENCES, VOL. 37, NOVEMBER 2020, 1211–1221

• **Original Paper** •

Establishment of an Objective Standard for the Definition of Binary Tropical Cyclones in the Western North Pacific

Fumin REN*[1,2], Yanjun XIE[3], Biwen YIN[4], Mingyang WANG[2], and Guoping LI[2]

[1]*State Key Laboratory of Severe Weather*, *Chinese Academy of Meteorological Sciences*, *Beijing* 100081, *China*

[2]*School of Atmospheric Sciences*, *Chengdu University of Information Technology*, *Chengdu* 610225, *China*

[3]*Zhuzhou Meteorological Observatory*, *Zhuzhou* 412000, *China*

[4]*Qinhuangdao Meteorological Observatory*, *Qinhuangdao* 066000, *China*

(Received 30 December 2019; revised 3 July 2020; accepted 7 July 2020)

ABSTRACT

To develop an objective standard for defining binary tropical cyclones (BTCs) in the western North Pacific (WNP), two best-track datasets, from the China Meteorological Administration and the Joint Typhoon Warning Center, were adopted for statistical analyses on two important characteristics of BTCs—two TCs approaching each other, and counterclockwise spinning. Based on the high consistency between the two datasets, we established an objective standard, which includes a main standard for defining BTCs and a secondary standard for identifying typical/atypical BTCs. The main standard includes two requirements: two coexisting TCs are a pair of BTCs if (i) the separation distance is ⩽ 1800 km, and (ii) this separation maintains for at least 12 h. Meanwhile, the secondary standard defines a typical BTC as one for which there is at least one observation when the two TCs approach each other and spin counterclockwise simultaneously. Under the standard, the ratio of typical BTCs increases as the BTC duration increases or the minimum distance between the two TCs decreases. Then, using the JTWC dataset, it was found that there are 505 pairs of BTCs during the period 1951–2014, including 328 typical BTCs and 177 atypical BTCs, accounting for 65.0% and 35.0% of the total, respectively. In addition, a study of two extreme phenomena—the maximum approaching speed and the maximum counterclockwise angular velocity in typical BTCs—shows that the configuration of the circulation conditions and the distribution of the BTCs favor the formation of these extreme phenomena.

Key words: objective standard, binary tropical cyclones, Western North Pacific

Citation: Ren, F. M., Y. J. Xie, B. W. Yin, M. Y. Wang, and G. P. Li, 2020: Establishment of an objective standard for the definition of binary tropical cyclones in the western North Pacific. *Adv. Atmos. Sci.*, **37**(11), 1211–1221, https://doi.org/10.1007/s00376-020-9287-3.

Article Highlights:

- An objective standard for the definition of BTCs in the WNP, which includes a main standard for defining BTCs and a secondary standard for identifying typical/atypical BTCs, has been established.
- The main characteristics of BTCs in the WNP are analyzed using the objective standard.
- Two extreme phenomena show that the configuration of the circulation conditions and the distribution of the BTCs favor the formation of the extreme phenomena.

1. Introduction

A binary vortex interaction, in which two cyclonic vortices at a relatively close range simultaneously perform a mutual counterclockwise spin and move closer to each other, is referred to as a binary tropical cyclone (BTC) and the Fujiwhara effect in honor of the pioneering work of Fujiwhara (1921, 1923, 1931). Chen and Ding (1979) pointed out that, when two TCs are enough close to each other, for either one, along the line between their centers, the pressure gradient force decreases suddenly on the side close to the other TC while the pressure gradient force remains the same on the opposite side. This situation is conducive to the two TCs approaching each other. Haurwitz (1951) studied the motion of BTCs and reported a method to compute the angular velocity of the rotation of the binary axis.

This typical motion of BTCs (the Fujiwhara effect) does not always occur when two TCs are close to each other (Hoover, 1961; Brand, 1970; Dong and Neumann, 1983;

* Corresponding author: Fumin REN
Email: fmren@163.com

Lander and Holland, 1993; Carr et al., 1997; Carr and Elsberry, 1998; Wu et al., 2011). Hoover (1961) reported that a separation distance of 600 nautical miles is the critical distance determining whether hurricane pairs in the Atlantic Ocean have the characteristics of BTCs, whereas Brand (1970) suggested that 750 nautical miles is the threshold separation distance in the western North Pacific (WNP). Lander and Holland (1993) showed that most interacting cyclones show four characteristic features: approach and capture, mutual orbit, merger, and escape. Rapid merger only occurs when BTCs approach within a critical separation distance, such as 150–300 km (Ritchie and Holland, 1993). Carr et al. (1997) proposed three modes for BTCs: direct interaction, semi-direct interaction, and indirect interaction. Carr and Elsberry (1998) carried out an objective diagnosis of the interactions of BTCs and presented objective criteria for distinguishing these three modes. BTCs have different manifestations because the relative motion of TC pairs is a function of both the Fujiwhara effect and differences in the large-scale environmental steering forces acting on each system (Brand, 1970; Dong and Neumann, 1983; Wang and Fu, 1983; Kuo et al., 2000; Wu et al., 2011). The significance of the Fujiwara effect in a TC pair depends on the distance between the two centers, the size, structure, and intensity of the two TCs, as well as the environmental steering currents (Brand, 1970).

Many different models have been proposed to explain the interactions of BTCs in terms of dynamics and thermodynamics (Chang, 1983; Holland and Dietachmayer, 1993; Falkovich et al., 1995; Wang and Holland, 1995; Khain et al., 2000; Prieto et al., 2003; Wu et al., 2003; Yang et al., 2008; Xu et al., 2011, 2013; Wu et al., 2012; Baumann et al., 2015; Liu and Tan, 2016; Xian and Chen, 2019). However, few studies have investigated the definition of BTCs and the criteria determining their formation.

There are three existing definitions of BTCs in the WNP. Brand (1970) used the following criteria to determine a valid binary system: (1) the TCs approach within 700 nautical miles (~1300 km) of each other at one point in time; (2) both storms occur over the open ocean; and (3) the storms must reach the intensity of a typhoon at one point in time. Moreover, Dong and Neumann (1983) defined a BTC as two TCs that: (1) have coexisted for at least 48 h; (2) were separated at some time by < 1334 km; and (3) attained at least tropical storm ($\geqslant$ 18 m s^{-1}) status. Meanwhile, a BTC has been defined by Wu et al. (2011) and Jang and Chun (2016) as two TCs that: (1) had attained at least tropical storm status; (2) were separated by a minimum distance < 1600 km; and (3) had coexisted for at least 48 h. However, although all these definitions use criteria based on the separation distance, TC intensity and the coexistence time, they are different from each other, and especially there does not exist any explanation or reason about the origins of those definitions. This means that the definitions are all mainly subjective and a generally accepted standard does not exist. It is not difficult to understand that this situation is very unfavorable for further in-depth research and operational application in this area. Therefore, a scientific issue arises as to whether we can establish an objective standard to define BTCs.

The motivation for this study is to develop an objective standard for defining BTCs in the WNP through carefully examining the observed interaction behavior between two coexisting TCs. We discuss the available data and our methods in section 2. Section 3 describes in detail how our standard is established. Using this standard, the main characteristics of BTCs are analyzed and presented in section 4. A summary and concluding remarks are given in the final section.

2. Data and methods

2.1. *Data*

Different datasets show clear differences in the intensity and location of TCs in the WNP basin (Yu et al., 2007; Knapp and Kruk, 2009; Song et al., 2010; Ren et al., 2011). We therefore used two different best-track datasets—one from the China Meteorological Administration (CMA) and the other from the Joint Typhoon Warning Center (JTWC)—to develop an objective standard for defining BTCs. Both datasets contain information on the six-hourly track and intensity of TCs in the period 1951–2014. We also used the monthly mean National Centers for Environmental Prediction reanalysis geopotential height dataset with a spatial resolution of 2.5° × 2.5° for the same period.

2.2. *Methods*

The basic features of BTCs are "mutual counterclockwise spinning and moving closer to each other" (Fujiwhara, 1921, 1923, 1931). We therefore designed a statistical analysis method to analyze the observations. Three parameters—the distance (d) between the centers of two coexisting TCs, the change in this distance (Δd), and the mutual angular velocity (r)—need to be calculated for any two coexisting TCs.

The value of d can be approximately calculated according to the formula for the distance between two points on a plane. Δd can be calculated as:

$$\Delta d_t = d_t - d_{t-1} \,, \tag{1}$$

where t is the number of records for two coexisting TCs and d_t and d_{t-1} represent the distances at time t and time t–1, respectively. $\Delta d < 0$ means that the two TCs are approaching each other, whereas $\Delta d > 0$ means that they are moving apart.

Figure 1 shows the schematic for calculating the mutual angular velocity between the two coexisting TCs. The value of r can be calculated as:

$$r_t = \theta_t - \theta_{t-1} \,, \tag{2}$$

where θ_t and θ_{t-1} represent the angles between the line connecting the two TCs and the weft at time t and time t–1,

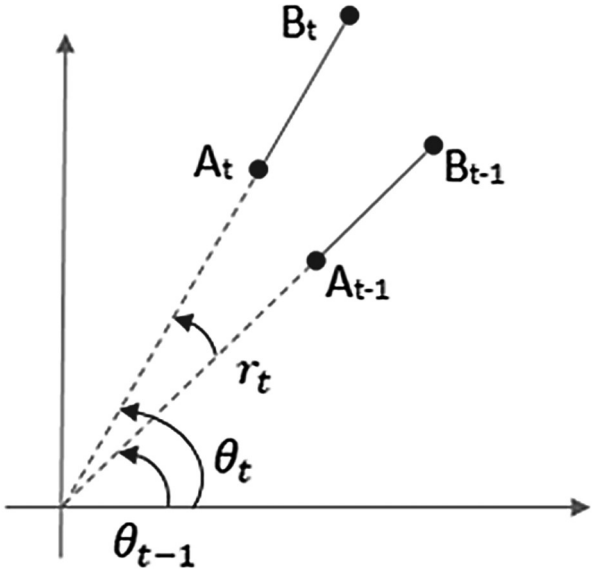

Fig. 1. Schematic for calculating the mutual angular velocity between two coexisting TCs.

respectively. $r_t > 0$ means that the rotation is counterclockwise, whereas $r_t < 0$ means that the rotation is clockwise.

Equations (1) and (2) show that calculations can only be performed when $t - 1 \geqslant 1$ (i.e. $t \geqslant 2$); that is, the duration $T \geqslant 12$ h ($12 = 2 \times 6$). Therefore, the duration of coexistence T should be at least 12 h and the three parameters only make sense when $t \geqslant 2$.

3. An objective standard for BTCs

Considering that the basic features of BTCs are "mutual counterclockwise spinning and moving closer to each other", we focus on the behavior of interaction between two coexisting TCs. Figure 2 presents frequency–distance distributions of two-TC coexistence for the CMA and the JTWC TC datasets. It can be seen that the frequencies in the two datasets both show a unimodal distribution with a peak at 2100 km, while the frequency in the JTWC dataset shows a weak secondary peak at 1900 km. In addition, as the CMA dataset contains more independent TCs than the JTWC dataset (Ren et al., 2011), the frequency of two coexisting TCs in the CMA dataset is greater than that in the JTWC dataset.

Figure 3 shows the ratio–distance distributions of TCs that are moving apart and approaching each other for the two datasets. The CMA dataset (Fig. 3a) shows that the ratio for two TCs approaching each other increases as the distance decreases, with a ratio of 0.387 at 3000 km and 0.701 at 500 km. By contrast, the ratio for two TCs that are moving apart decreases as the distance decreases. The two ratio lines intersect over a range from 1800 to 2300 km, in which the ratios for both TCs approaching each other and TCs that are moving apart oscillate around 0.5, which means that the probabilities of occurrences for approaching and escaping are equivalent. The JTWC dataset (Fig. 3b) shows similar features with the same range of intersection. The range of intersection means that within a separation distance of 1800 km, the ratio for TCs approaching each other is > 0.5, which means that the probability of occurrence for approaching becomes dominant and increases as the distance decreases.

Figure 4 depicts the counterclockwise and clockwise ratio–distance distributions and can be used to examine the mutual angular velocity between two coexisting TCs. The JTWC dataset (Fig. 4b) shows that the counterclockwise ratio increases as the distance decreases, with a ratio of 0.416 at 3000 km and 0.846 at 500 km. By contrast, the clockwise ratio decreases as the distance decreases, with a ratio

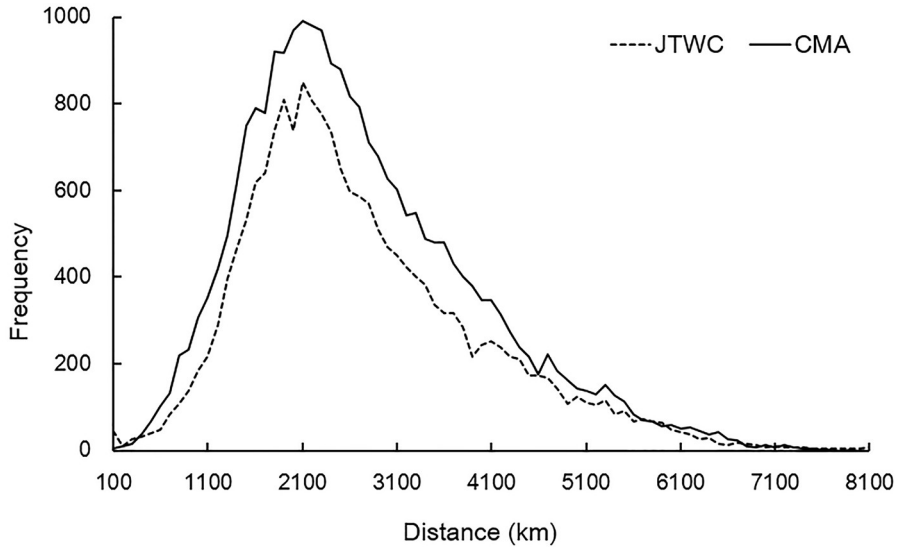

Fig. 2. Frequency–distance distributions of two-TC coexistence for the CMA and the JTWC TC datasets. Here, "distance" is the amount of space between two TC centers, while "frequency" means the number of TC pairs. The distance interval for the statistics is 100 km, with the maximum value representing the interval, e.g., 1500 for (1400, 1500].

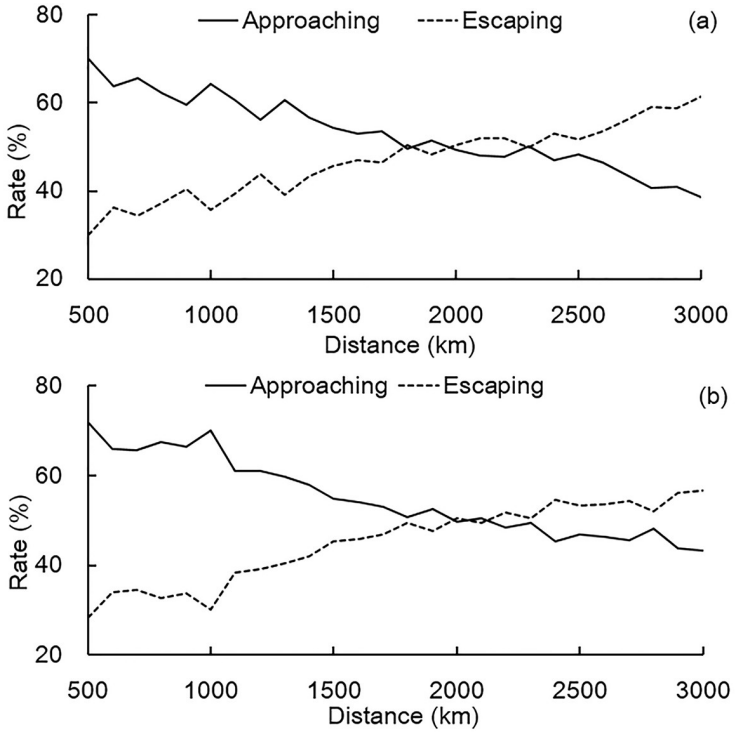

Fig. 3. Approaching and escaping ratio–distance distributions of two TCs coexisting in the CMA and the JTWC datasets. Here, "ratio" means the ratio of number of coexisting TC pairs approaching or escaping to the total number of coexisting TC pairs. The distance interval for the statistics is 100 km, with the maximum value representing the interval, e.g., 1500 for (1400, 1500]. (a) CMA dataset. (b) JTWC dataset.

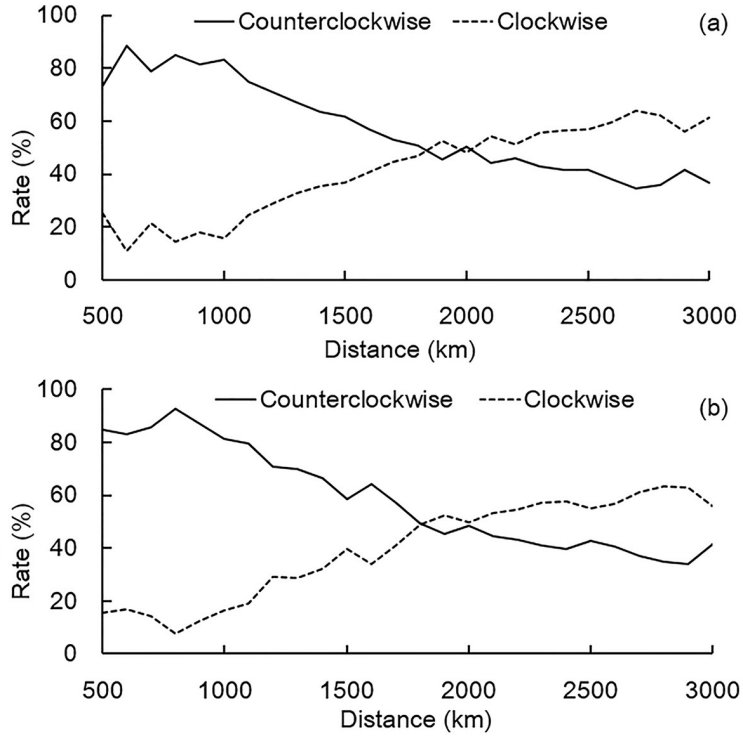

Fig. 4. As in Fig. 3 but for counterclockwise and clockwise ratio–distance distributions. Here, "ratio" indicates the ratio of number of coexisting TC pairs with counterclockwise rotation or clockwise rotation to the total number of coexisting TC pairs. (a) CMA dataset. (b) JTWC dataset.

of 0.558 at 3000 km and 0.154 at 500 km. The counterclockwise and clockwise ratios intersect over a range from 1800 to 2000 km, in which both ratios oscillate around 0.5, which means that the probabilities of occurrences for counterclockwise and clockwise are equivalent. The CMA dataset (Fig. 4a) also displays highly consistent features with the same range of intersection. The intersection range also means that within a separation distance of 1800 km, the counterclockwise ratio is > 0.5, which means that the probability of occurrence for counterclockwise becomes dominant and increases as the distance decreases.

Based on these analyses, the two datasets both show that 1800 km is a key distance in defining BTCs: within a separation distance of 1800 km, the approaching ratio and counterclockwise ratio are both > 0.5 and increase as the distance decreases. As a result, 1800 km was selected as the threshold distance to define a BTC in Eq. (3). Taking into consideration the requirement for the duration T in Eq. (4), an objective standard for a BTC in the WNP can be established. If the distance between the centers of two coexisting TCs is $\leqslant d_0$ (1800 km) and the duration is at least 12 h, then they can be defined as a BTC:

$$d \leqslant d_0 \,, \tag{3}$$

$$T = m\Delta t \,, \tag{4}$$

where Δt is the time interval (6 h) between two adjacent observations of a tropical cyclone and m ($m \geqslant 2$) is the number of consecutive observations with $d \leqslant d_0$.

The distance threshold, 1800 km, which is larger than those of the three existing definitions of BTCs, is a key parameter in the objective standard. The distance between the centers of the two TC centers defines 900 km as an important TC size. According to Chavas et al. (2016), the median and mean sizes of the outer radius of a TC in the WNP are 957.6 and 993.5 km, respectively. These three TC sizes are clearly of the same order of magnitude. This suggests that the distance threshold, 1800 km, can be understood to be twice the mean outer radius within which two TCs easily interact with each other and show clear characteristics of BTCs.

Our results are consistent with previous studies (Brand, 1970; Dong, 1980, 1981; Dong and Neumann, 1983; Kuo et al., 2000; Wu et al., 2011) in which the significance of the Fujiwara effect in a pair of TCs is dependent on the distance between the centers of two TCs. Other factors include the size, structure, and the intensity of the two TCs, as well as the environmental steering currents.

However, an approaching ratio and counterclockwise ratio both > 0.5 does not mean that the two TCs will simultaneously perform a mutual counterclockwise spin and approach each other. It is necessary to introduce a secondary standard to distinguish whether a particular example is a typical BTC. For this purpose, we consider two different conditions: (1) there is at least one observation of $\Delta d < 0$ and at least one observation of $r_t > 0$ during the duration of the BTC; and (2) there is at least one simultaneous observation of both $\Delta d < 0$ and $r_t > 0$ during the duration of the BTC. Table 1 presents the statistics of typical BTCs with the two different conditions. It is revealed that, though the BTC frequencies are considerably different between the CMA and JTWC datasets, the typical BTC ratios are highly consistent with each other, being 0.680–0.689 under condition 1 and 0.642–0.650 under condition 2. Based on the comparison, condition 2, which means both $\Delta d < 0$ and $r_t > 0$ are observed simultaneously, and the ratios under which for the CMA and JTWC datasets are more consistent than those under condition 1, is selected as the standard for defining typical BTCs. Accordingly, a BTC that does not satisfy condition 2 is defined as an atypical BTC.

4. Main characteristics of BTCs under the objective standard

Under the objective standard defined by Eqs. (3) and (4) and the secondary standard of condition 2, the JTWC dataset was adopted to analyze the characteristics of BTCs. As shown in Table 1, there are 505 pairs of BTCs in the WNP during the period 1951–2014, with 328 pairs of typical BTCs and 177 pairs of atypical BTCs accounting for 65.0% and 35.0% of the total, respectively.

We considered two statistical variables in detail: the duration of the BTC and the minimum distance between the centers of the two TCs during the duration of the BTC. The duration varied from 12 to 264 h and Fig. 5a shows the variations in the ratios for the duration of the two types of BTC. The ratio for a typical BTC is smaller than that for an atypical BTC only when the duration is < 24 h. The ratio is 0.28 at 12 h, increases rapidly between 12 and 84 h, and then varies in the range 0.80–1.0, with the value always being 1.0 when the duration of the BTC is ⩾ 144 h. The minimum distance changes from 133.5 to 1800 km and Fig. 5b presents the variation in the ratios at the minimum distance for the two types of BTC. The ratio for a typical BTC increases as the minimum distance decreases and is smaller than that of an atypical BTC when the minimum distance is between 1700 and 1800 km. The ratio is 0.37 at 1800 km and is larger than that of an atypical BTC when the minimum distance is < 1700 km, with a value of 1.0 at ⩽ 300 km.

Figure 6 depicts annual variations of frequencies for the two types of BTC over the WNP during the period

Table 1. Statistics of typical BTCs with two different phenomena. Condition 1: at least one observation of $\Delta d < 0$ and at least one observation of $r_t > 0$ exists during the BTC's duration. Condition 2: at least one observation of both $\Delta d < 0$ and $r_t > 0$ exists simultaneously during the BTC's duration.

	CMA		JTWC	
	Frequency	Ratio	Frequency	Ratio
Condition 1	481	0.680	348	0.689
Condition 2	454	0.642	328	0.650
BTC	707	–	505	–

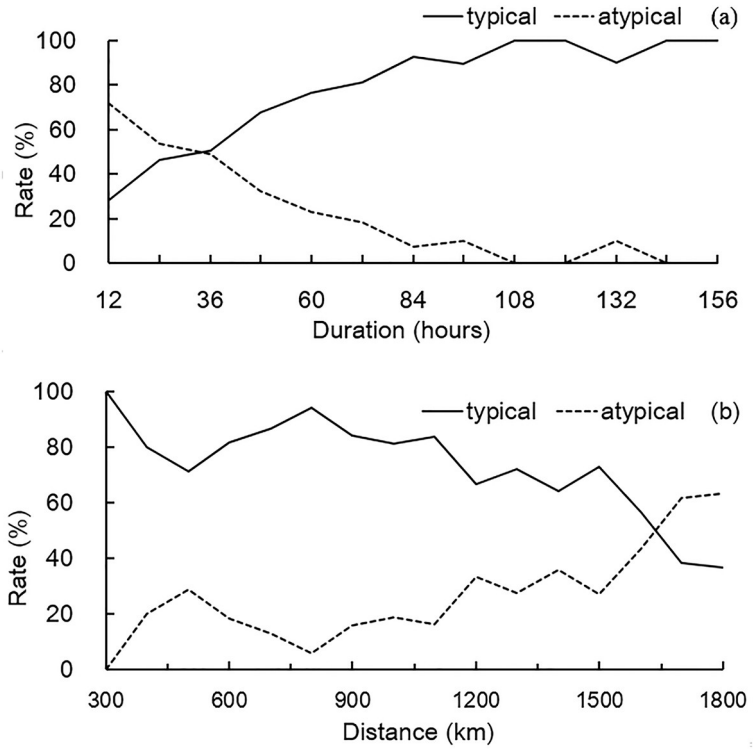

Fig. 5. Variations of rates of different variables for the two types of BTC over the WNP during the period 1951–2014: (a) duration of BTCs; (b) minimum distance between the two TCs during the duration of BTCs.

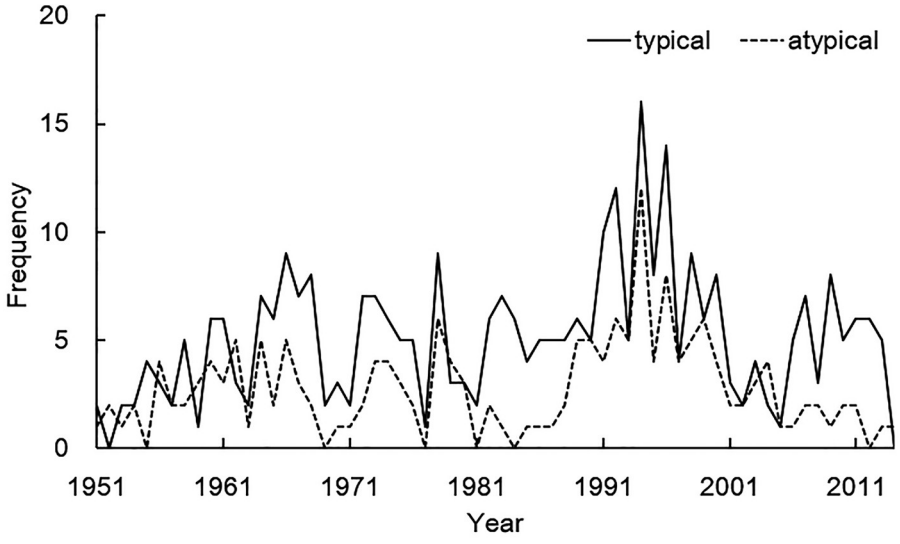

Fig. 6. Annual variations of frequencies for the two types of BTC over the WNP during the period 1951–2014.

1951–2014. During 1951–2014, the frequency of typical BTC mainly shows an obvious interdecadal variation, with large values during the 1990s and the maximum 16 in 1994, but values of zero in 1952 and 2014. Meanwhile, the frequency of atypical BTCs also indicates a similar interdecadal variation. The above interdecadal variations with large values during the 1990s in the two types of BTC are consistent with the variations in TC number and intensity in the JTWC dataset during that period (Ren et al., 2011). Ren et al. (2011) pointed out that the TC number and intensity in the JTWC dataset seems to be overestimated since 1988, particularly from 1993 to 2003, with the possible factors being as follows: (i) no TC intensity references with high accuracy for operational centers after aircraft reconnaissance terminated in 1987; (ii) obvious differences in applications of the Dvorak technique in different operational typhoon/hurricane centers; and (iii) differences in time intervals for the maximum sustained wind speed (MSWS) at different cen-

ters, especially when in-situ observation was available.

Figure 7 presents the seasonal variations of frequencies for the total and the two types of BTCs. It clearly shows that about 93.5% occur during June to November, with the most active season between July and September, but especially August, in which 67.3% occur. Meanwhile, BTCs rarely appear in May, December and January, while no BTC occurs from February to April.

For each BTC pair, there might exist two (different) numbers of times for approaching each other or counterclockwise rotation. Among each of the two numbers, two extreme phenomena are of particular interest: the maximum approaching speed (extreme phenomenon 1) and the maximum counterclockwise angular velocity (extreme phenomenon 2) between the two TCs. To study the characteristics of typical BTCs with these two extreme phenomena during the active season from July to September, a statistic was derived for the direction of the line segment between the two TCs. It is easy to understand that θ, as defined in section 2, satisfies the relation $180° > \theta \geqslant 0°$. Six directions are applied in the statistics: direction 1 ($30° > \theta \geqslant 0°$), direction 2 ($60° > \theta \geqslant 30°$), direction 3 ($90° > \theta \geqslant 60°$), direction 4 ($120° > \theta \geqslant 90°$), direction 5 ($150° > \theta \geqslant 120°$), and direction 6 ($180° > \theta \geqslant 150°$). The results of the above statistics show that, with extreme phenomenon 1, direction 1 (35.0%) and direction 6 (28.3%) are the two most frequent directions, with a total frequency ratio of 63.3%. By contrast, with extreme phenomenon 2, direction 1 (37.2%) and direction 2 (17.9%) are the two most frequent directions, with a total frequency ratio of 55.1%.

Figure 8a shows the distributions of the BTC locations in the two most frequent directions, their mean position with extreme phenomenon 1, and the average position of subtropical highs during the period July–September. The mean position of BTCs shows a west–east direction, with the center of the western TC at (21.8°N, 127.0°E) and the center of the eastern TC at (22.0°N, 142.1°E), with a separation distance of 1557.3 km. The average position of the subtropical high clearly benefits the formation of extreme phenomenon 1. With these phenomena, the BTC is mainly controlled by an easterly stream along the southern edge of the subtropical high and the eastern TC moves rapidly toward the western TC under the guiding easterly airflow.

Figure 8b depicts similar characteristics to Fig. 8a, but for extreme phenomenon 2. The mean position of the BTC shows movement from the northeast to southwest, with the center of the western TC locating at (21.3°N, 127.1°E) and the center of the eastern TC locating at (25.6°N, 139.0°E), with a separation distance of 1303.9 km. The location of the subtropical high clearly benefits the formation of extreme phenomenon 2. At the moment, the BTC is mainly distributed in a northeast to southwest direction, with the eastern TC locating at the southwestern edge of the subtropical high and being controlled by the southeasterly stream, thus favoring counterclockwise spinning between the BTCs.

In order to compare the differences of the large-scale weather systems associated with the two type BTCs, representative samples for typical and atypical BTCs were chosen from the BTCs with the intensity of the stronger TC $\geqslant$ 32.7 m s^{-1} and that of the weaker TC < 32.7 m s^{-1}, as follows: (i) typical BTCs: the first moment when BTCs simultaneously show approaching and spinning counterclockwise for the typical BTCs in the two most frequent directions during July–September; and (ii) atypical BTCs: the moment when BTCs are at the minimum distance during the duration of the atypical BTCs in the two most frequent directions during July–September. Figure 9 shows the distributions of the locations of the representative samples for typical and atypical BTCs. Figure 9a shows that the mean position of representative typical BTCs shows a slightly northeast–southwest direction, with the center of the western TC at (20.9°N, 127.8°E), the center of the eastern TC at (21.5°N, 142.5°E), and a separation distance of 1521.3 km. Based on the analyses of Fig. 8 it is easy to understand that the configuration of the subtropical high and the representative typical BTCs clearly benefits the occurrence of BTCs sim-

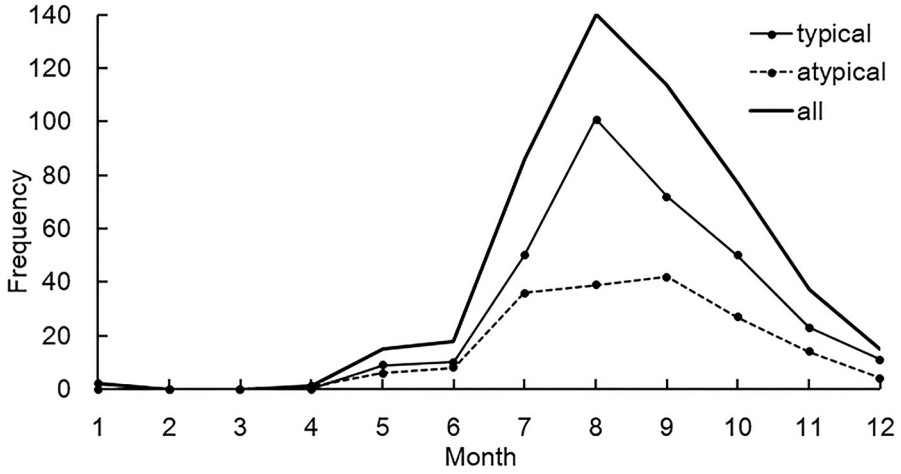

Fig. 7. Seasonal variations of frequencies for the total and the two types of BTCs over the WNP during the period 1951–2014.

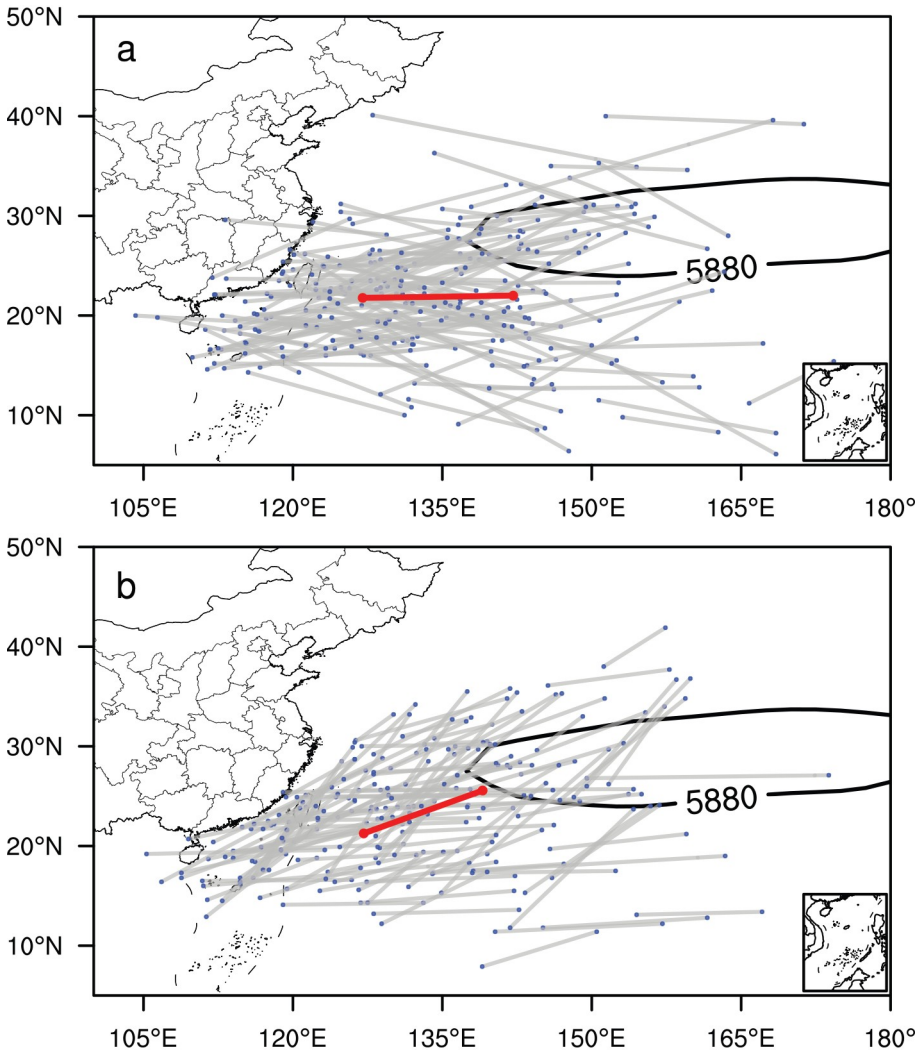

Fig. 8. Positions of typical BTCs (two blue dots connected by gray line segments) in the two most frequent directions and their mean position (the two red dots connected by a red line segment) with two different extreme phenomena during the duration of BTCs and the average position of the subtropical high during the period of frequent BTCs (July–September) over the WNP from 1951 to 2014 using the monthly mean geopotential height from the NCEP reanalysis dataset: (a) maximum speed of approaching toward each other; (b) maximum counterclockwise angular velocity.

ultaneously approaching and spinning counterclockwise. Meanwhile, Fig. 9b indicates that the mean position of representative atypical BTCs shows an obvious northwest–southeast direction, with the western TC at (27.7°N, 128.1°E), the center of the eastern TC at (20.2°N, 139.8°E), and a separation distance of 1452.2 km. Taking into consideration that the western TC generally locates in the monsoon trough (figure omitted), which is mainly west of the mean position of representative atypical BTCs, the configuration of the subtropical high, the monsoon trough and the representative atypical BTCs does not benefit the occurrence of BTCs approaching or spinning counterclockwise.

5. Summary and concluding remarks

The following conclusions can be drawn based on our analyses.

An objective standard to define BTCs has been established based on statistical observations of TCs in the WNP. The objective standard includes a main standard for defining BTCs and a secondary standard for defining typical/atypical BTCs. The main standard has two requirements: two coexisting TCs are a pair of BTCs if (i) the separation distance is $\leqslant$ 1800 km, and (ii) this separation maintains for at least 12 h. The secondary standard defines a typical BTC as one for which there is at least one observation when the two TCs approach each other and spin counterclockwise simultaneously; otherwise they are atypical BTCs.

There are 505 pairs of BTCs during the period 1951–2014, including 328 typical BTCs and 177 atypical BTCs, accounting for 65.0% and 35.0% of the total, respectively. The duration of the BTCs varies from 12 to 264 h and

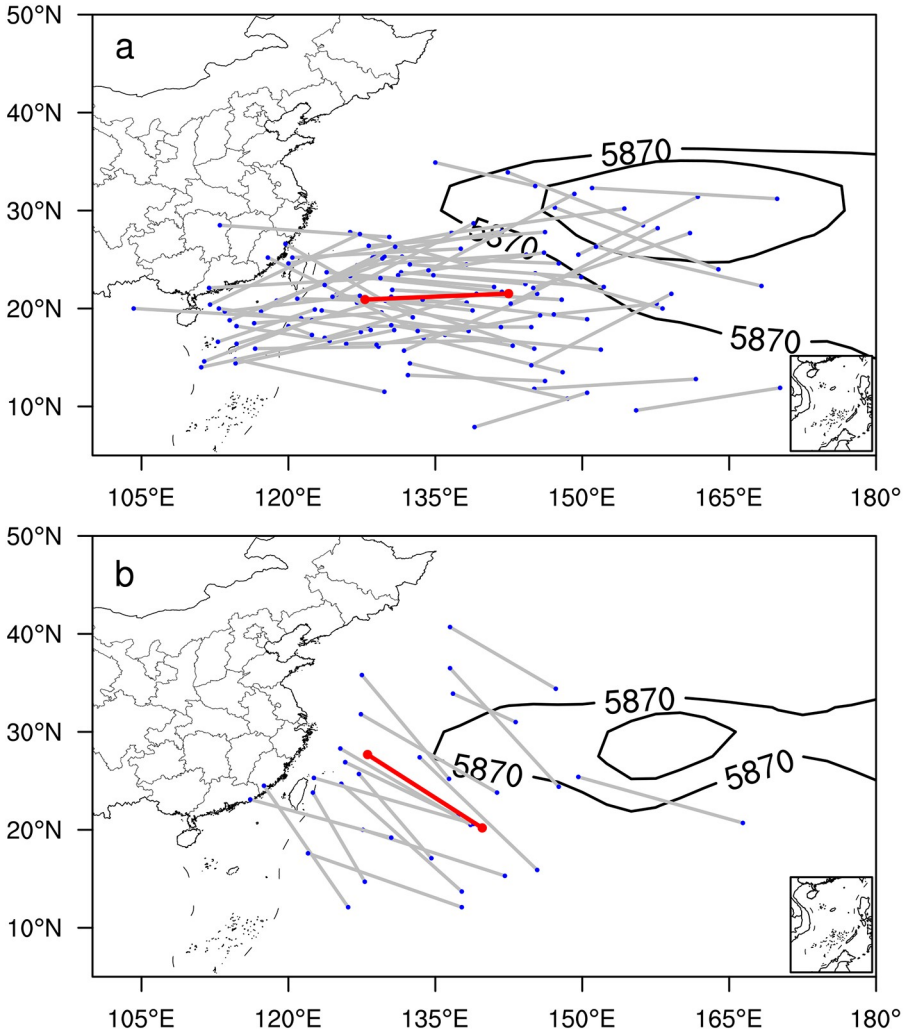

Fig. 9. As in Fig. 8 but for representative samples for (a) typical and (b) atypical BTCs in the two most frequent directions and their mean positions. Typical BTCs are selected at the first moment when BTCs simultaneously show approaching and spinning counterclockwise during July–September, while atypical BTCs are chosen at the moment when BTCs are at the minimum distance during the same period. The subtropical high is the average position of subtropical highs at corresponding moments.

the minimum distance is in the range 133.5–1800 km. The ratio of typical BTCs increases as the duration increases, with the value always being 1.0 when the duration is ⩾ 144 h. The ratio increases as the minimum distance decreases, with the value always being 1.0 at ⩽ 300 km.

A study of the two extreme phenomena for typical BTCs shows that the configurations of the circulation conditions and the distribution of the BTC favor the formation of the extreme phenomena. At the time of the maximum approaching speed, when the BTCs are mainly located along the southern edge of the subtropical high, the movement of the eastern TC toward the western TC can be increased under the easterly steering airflow. At the time of the maximum counterclockwise angular velocity, the BTCs are mainly distributed in a northeast–southwest direction, with the eastern TC locating at the southwestern edge of the subtropical high and being controlled by the southeasterly stream. This favors anticlockwise spinning between the two TCs.

In order to understand more clearly the merits of our BTC-identification standard compared to the previous BTC definitions, the differences can be summarized in two aspects: First, our standard is objective, while the previous BTC definitions are mainly subjective. Our standard is based on statistical analyses of two best-track datasets, CMA and JTWC, with the separation distance of ⩽ 1800 km between the centers of two TCs equating to two times the average size of the TC outer radius in the WNP. Meanwhile, the previous BTC definitions do not provide any explanation or reason regarding the origins of the definitions. Second, our standard has a secondary standard for identifying typical/atypical BTCs, whereas the previous BTC definitions do not. Under our standard, a smaller minimum distance between the two TCs or a longer duration of interaction gives a larger proportion of typical BTCs. Meanwhile, it is notable that about 35.0% (= 177 / 505) of total

BTCs are atypical BTCs that do not have any moment where they are simultaneously approaching each other and spinning counterclockwise, especially at short distances with a certain ratio of BTCs moving apart and rotating clockwise. These situations might indicate the environmental effects on BTC behavior.

A number of new issues arise from this study. For example, are there any differences between our standard in the WNP and standards in other TC basins in the Southern Hemisphere? BTCs often produce extreme rainfall events resulting in serious damage—for example, Typhoon Morakot in Taiwan in 2009 and Typhoon Fitow in Zhejiang in 2013 in China were both the result of BTCs. However, we do not have a clear picture of the characteristics of BTC interactions in China's offshore area. These issues require further in-depth studies.

Acknowledgements. The authors would like to express their sincere thanks to the three anonymous reviewers and the editor for their helpful suggestions and comments to improve the manuscript. This work was supported by the National Natural Science Foundation of China (Grant No. 41675042) and the Jiangsu Collaborative Innovation Center for Climate Change. We acknowledge the use of the best-track datasets from the CMA and JTWC, and the monthly mean geopotential height from the NCEP reanalysis dataset.

REFERENCES

Baumann, M., V. Heuveline, L. Scheck, and S. C. Jones, 2015: Goal-oriented adaptivity for idealised tropical cyclones: A binary interaction scenario. *Meteor. Z.*, **24**, 269–292, https://doi.org/10.1127/metz/2015/0591.

Brand, S., 1970: Interaction of binary tropical cyclones of the western North Pacific Ocean. *J. Appl. Meteorol.*, **9**, 433–441, https://doi.org/10.1175/1520-0450(1970)009<0433:IOBTCO>2.0.CO;2.

Carr, L. E., M. A. Boothe, and R. L. Elsberry, 1997: Observational evidence for alternate modes of track-altering binary tropical cyclone scenarios. *Mon. Wea. Rev.*, **125**, 2094–2111, https://doi.org/10.1175/1520-0493(1997)125<2094:OEFAMO>2.0.CO;2.

Carr, L. E., and R. L. Elsberry, 1998: Objective diagnosis of binary tropical cyclone interactions for the Western North Pacific Basin. *Mon. Wea. Rev.*, **126**, 1734–1740, https://doi.org/10.1175/1520-0493(1998)126<1734:ODOBTC>2.0.CO;2.

Chang, S. W.-J., 1983: A numerical study of the interactions between two tropical cyclones. *Mon. Wea. Rev.*, **111**, 1806–1817, https://doi.org/10.1175/1520-0493(1983)111<1806:ANSOTI>2.0.CO;2.

Chavas, D. R., N. Lin, W. H. Dong, and Y. L. Lin, 2016: Observed tropical cyclone size revisited. *J. Climate*, **29**, 2923–2939, https://doi.org/10.1175/JCLI-D-15-0731.1.

Chen, L. S., and Y. H. Ding, 1979: *Generality of Western Pacific Typhoon*. Science Press, 221 pp. (in Chinese)

Dong, K., 1980: The phenomena and reasons for close binary Typhoons mutually rotate clockwise. *Meteorological Monthly*, **6**(6), 18–19. (in Chinese)

Dong, K., 1981: Analysis on 6413–6414 binary typhoons mutually rotating and merging. *Acta Meteorologica Sinica*, **39**(3), 361–370. (in Chinese)

Dong, K. Q., and C. J. Neumann, 1983: On the relative motion of binary tropical cyclones. *Mon. Wea. Rev.*, **111**, 945–953, https://doi.org/10.1175/1520-0493(1983)111<0945:OTRMOB>2.0.CO;2.

Falkovich, A. I., A. P. Khain, and I. Ginis, 1995: Motion and evolution of binary tropical cyclones in a coupled atmosphere-ocean numerical model. *Mon. Wea. Rev.*, **123**, 1345–1363, https://doi.org/10.1175/1520-0493(1995)123<1345:MAEOBT>2.0.CO;2.

Fujiwhara, S., 1921: The natural tendency towards symmetry of motion and its application as a principle in meteorology. *Quart. J. Roy. Meteor. Soc.*, **47**, 287–293, https://doi.org/10.1002/qj.49704720010.

Fujiwhara, S., 1923: On the growth and decay of Vortical systems. *Quart. J. Roy. Meteor. Soc.*, **49**, 75–104, https://doi.org/10.1002/qj.49704920602.

Fujiwhara, S., 1931: Short note on the behavior of two vortices. *Proceedings of the Physico-Mathematical Society of Japan. 3rd Series*, **13**, 106–110, https://doi.org/10.11429/ppmsj1919.13.3_106.

Haurwitz, B., 1951: The motion of binary tropical cyclones. *Archiv für Meteorologie, Geophysik und Bioklimatologie, Serie A*, **4**, 73–86, https://doi.org/10.1007/BF02246794.

Holland, G. J., and G. S. Dietachmayer, 1993: On the interaction of tropical-cyclone-scale vortices. III: Continuous barotropic vortices. *Quart. J. Roy. Meteor. Soc.*, **119**, 1381–1398, https://doi.org/10.1002/qj.49711951408.

Hoover, E. W., 1961: Relative motion of hurricane pairs. *Mon. Wea. Rev.*, **89**, 251–255, https://doi.org/10.1175/1520-0493(1961)089<0251:RMOHP>2.0.CO;2.

Jang, W., and H.-Y. Chun, 2016: Characteristics of binary tropical cyclones observed in the western north pacific for 62 Years (1951-2012). *Mon. Wea. Rev.*, **143**, 1749–1761, https://doi.org/10.1175/MWR-D-14-00331.1.

Khain, A., I. Ginis, A. Falkovich, and M. Frumin, 2000: Interaction of binary tropical cyclones in a coupled tropical cyclone-ocean model. *J. Geophys. Res.*, **105**, 22337–22354, https://doi.org/10.1029/2000JD900268.

Knapp, K. R., and M. C. Kruk, 2009: Quantifying interagency differences in tropical cyclone best-track wind speed estimates. *Mon. Wea. Rev.*, **138**(4), 1459–1473.

Kuo, H.-C., G. T.-J. Chen, and C.-H. Lin, 2000: Merger of tropical cyclones Zeb and Alex. *Mon. Wea. Rev.*, **128**, 2967–2975, https://doi.org/10.1175/1520-0493(2000)128<2967:MOTCZA>2.0.CO;2.

Lander, M., and G. J. Holland, 1993: On the interaction of tropical-cyclone-scale vortices. I: Observations. *Quart. J. Roy. Meteor. Soc.*, **119**, 1347–1361, https://doi.org/10.1002/qj.49711951406.

Liu, H.-Y., and Z.-M. Tan, 2016: A dynamical initialization scheme for binary tropical cyclones. *Mon. Wea. Rev.*, **144**, 4787–4803, https://doi.org/10.1175/MWR-D-16-0176.1.

Prieto, R., B. D. Mcnoldy, S. R. Fulton, and W. H. Schubert, 2003: A classification of binary tropical cyclone-like vortex interactions. *Mon. Wea. Rev.*, **131**, 2656–2666, https://doi.org/10.1175/1520-0493(2003)131<2656:ACOBTC>2.0.CO;2.

Ren, F. M., J. Liang, G. X. Wu, W. J. Dong, and X. Q. Yang, 2011: Reliability analysis of climate change of tropical cyclone activity over the Western North Pacific. *J. Climate*, **24**, 5887–5898, https://doi.org/10.1175/2011JCLI3996.1.

Ritchie, E. A., and G. J. Holland, 1993: On the interaction of tropical-cyclone-scale vortices. II: Discrete vortex patches. *Quart. J. Roy. Meteor. Soc.*, **119**, 1363–1379, https://doi.org/10.1002/qj.49711951407.

Song, J.-J., Y. Wang, and L. G. Wu, 2010: Trend discrepancies among three best track data sets of western North Pacific tropical cyclones. *J. Geophys. Res.*, **115**, D12128, https://doi.org/10.1029/2009JD013058.

Wang, Y. Q., and G. J. Holland, 1995: On the interaction of tropical-cyclone-scale vortices. IV: Baroclinic vortices. *Quart. J. Roy. Meteor. Soc.*, **121**, 95–126, https://doi.org/10.1002/qj.49712152106.

Wang, Z., and X. Fu, 1983: The Interaction of Binary Typhoons and its influence on their movements. *Chinese Journal of Atmospheric Sciences*, **7**(3), 269–276. (in Chinese)

Wu, C.-C., T.-S. Huang, W.-P. Huang, and K.-H. Chou, 2003: A new look at the binary interaction: Potential Vorticity diagnosis of the unusual southward movement of tropical storm Bopha (2000) and its interaction with Supertyphoon Saomai (2000). *Mon. Wea. Rev.*, **131**, 1289–1300, https://doi.org/10.1175/1520-0493(2003)131<1289:ANLATB>2.0.CO;2.

Wu, X., J.-F. Fei, X. G. Huang, X.-P. Cheng, and J.-Q. Ren, 2011: Statistical classification and characteristics analysis of binary tropical cyclones over the Western North Pacific Ocean. *J. Trop. Meteor.*, **17**, 335–344, https://doi.org/10.3969/j.issn.1006-8775.2011.04.003.

Wu, X., J. F. Fei, X. G. Huang, X. Zhang, X. P. Cheng, and J. Q. Ren, 2012: A numerical study of the interaction between two simultaneous storms: Goni and Morakot in September 2009. *Adv. Atmos. Sci.*, **29**, 561–574, https://doi.org/10.1007/s00376-011-1014-7.

Xian, Z. P., and K. Y. Chen, 2019: Numerical analysis on the effects of binary interaction between typhoons Tembin and Bolaven in 2012. *Advances in Meteorology*, 7529263, https://doi.org/10.1155/2019/7529263.

Xu, X. D., C. Lu, H. X. Xu, and L. S. Chen, 2011: A possible mechanism responsible for exceptional rainfall over Taiwan from Typhoon Morakot. *Atmos. Sci. Lett.*, **12**, 294–299, https://doi.org/10.1002/asl.338.

Xu, H. X., X. J. Zhang, and X. D. Xu, 2013: Impact of tropical storm Bopha on the intensity change of super typhoon Saomai in the 2006 typhoon season. *Advances in Meteorology*, Article ID 487010, https: //doi.org/10.1155/2013/487010.

Yang, C.-C., C.-C. Wu, K.-H. Chou, and C.-Y. Lee, 2008: Binary interaction between Typhoons Fengshen (2002) and Fungwong (2002) based on the potential vorticity diagnosis. *Mon. Wea. Rev.*, **136**, 4593–4611, https://doi.org/10.1175/2008MWR2496.1.

Yu, H., C. M. Hu, and L. Y. Jiang, 2007: Comparison of three tropical cyclone intensity datasets. *Acta Meteorologica Sinica*, **21**, 121–128.